AIAA SciTech Forum
4-8 January 2016, San Diego, California, USA
34th Wind Energy Symposium

10.2514/6.2016-1997

An Experimental Investigation on the Aeromechanic Performance and Wake Characteristics of a Wind Turbine Model Subjected to Pitch Motions

Morteza Khosravi[1], Partha Sarkar[2], Hui Hu[3](✉)

Iowa State University, Ames, Iowa, 50011

In the present study, an experimental study was performed to analyze the loading, performance, and the near wake characteristics of a wind turbine model subjected to pitch motions. The experimental study was performed in a large-scale atmospheric boundary layer wind tunnel with a scaled three-bladed Horizontal Axial Wind Turbine model placed in turbulent boundary layer airflow with similar mean and turbulence characteristics as those over a typical offshore wind farm. The base of the 1:300 scaled model wind turbine was mounted on a translation and rotation stage in pitch motions to simulate the dynamic pitching motions experienced by floating offshore wind turbines. A high resolution digital particle image velocimetry (PIV) system was used to achieve flow field measurements to quantify the characteristics of the turbulent vortex flow in the near wake of the wind turbine model. The effects of the pitch motions of the wind turbine base on the turbine wake characteristics were examined in details based on the PIV measurements. The power production performance of the scaled model wind turbine was measured by using a small DC motor mounted inside the turbine nacelle assembly. A highly sensitive force/moment transducer was also used to measure the aerodynamic loading associated with the pitching turbine. The measurement results were compared to those of a bottom fixed turbine in order to evluate the effects of the pitching motions on the aeromechanic performance and wake characteristics of floating wind turbines sited in offshore wind farms

I. Introduction

Due to stronger wind speeds at lower altitudes and lower ambient turbulence, floating wind turbines in deep water offshore environments can be beneficial in terms of higher energy production and lower fatigue loads on the turbines. However, there are significant technological challenges associated with floating wind turbines in deep waters. The dynamic excitation of wind and waves can induce excessive motions along each of the 6 degrees of freedom (6-DOF) of the floating platforms. These motions will then be transferred to the turbine, and directly impact the loading, performance, and the wake characteristics of the floating wind turbines in an offshore environment

In the present study, a comprehensive experimental study was performed to analyze the loading, performance, and the near wake characteristics of a wind turbine model subjected to uncoupled pitch motions. These experimental studies were performed in a large-scale atmospheric boundary layer wind tunnel with a scaled three-bladed Horizontal Axial Wind Turbine model placed in a turbulent boundary layer airflow with similar mean and turbulence characteristics as those over a typical offshore wind farm. The base of the 1:300 scaled model wind turbine was mounted on a rotation stage. The rotation stage can be controlled to generate pitch motions to simulate the dynamics of pitching motions experienced by floating offshore wind turbines

A high resolution digital particle image velocimetry (PIV) system was used to achieve flow field measurements to quantify the characteristics of the turbulent vortex flow in the near wake of the wind turbine model. Besides conducting ‘‘free run’’ PIV measurements to determine the ensemble-averaged statistics of the flow quantities such

[1] Graduate Student, Department of Aerospace Engineering.
[2] Professor, Department of Aerospace Engineering.
[3] Professor, Department of Aerospace Engineering, AIAA Associate Fellow, Email: huhui@iastate.edu

as mean velocity, Reynolds stress, and turbulence kinetic energy (TKE) distributions in the wake flow, ‘‘phase-locked’’ PIV measurements were also performed to elucidate further details about evolution of the unsteady vortex structures in the wake flow in relation to the position of the rotating turbine blades. The effects of the pitch motions of the wind turbine base on the wake flow characteristics were examined in great details based on the PIV measurements. The performance of the scaled model wind turbine was measured using a small DC motor mounted in the nacelle assembly. A highly sensitive force/moment transducer was also mounted at the base of the turbine to measure the aerodynamic loading associated with the pitching turbine. For better understanding of the effects of pitching motion on the Aerodynamics and Aeromechanics of wind turbines, the results were then compared to those of a traditional bottom fixed turbine

The results of the wake studies reveal that the wake of a wind turbine subjected to pitch motions, is highly dependent on which direction the turbine is oscillating. Furthermore, the velocity, frequency, and the range of oscillation also play an important role on the behavior and the wake pattern of the moving turbine. In the case of the pitching turbine, the wake accelerates as the turbine is moving with the flow, hence, reducing the power extraction by the turbine. A decrease in Reynolds shear stress and the turbulent kinetic energy production was noted as the turbine was oscillating with the flow. However, as the turbine was moving into the flow, these effects reverse, and causes a deceleration in the wake of the moving turbine, hence increases the power production by the turbine, and increases the Reynolds shear stress and the turbulent kinetic energy. The mean power measurement using a small DC motor mounted in the nacelle, show little difference between the power extracted by turbine in pitch motion and the bottom fixed turbine. However, the fluctuations in the power output of the pitching turbine is greatly influcing the quality of power generated by such turbines. The mean thrust load experienced by both turbines are also quite similar. However, the fluctuations in the thrust loading experienced by the pitching turbine is much more than the bottom fixed turbine, hence increases the fatigue loads experienced by the pitching turbine.

II. Experimental Setup

The present experimental study was performed at the large-scale Aerodynamic/Atmospheric Boundary Layer (AABL) wind and gust tunnel located in the Department of Aerospace Engineering at Iowa State University. The AABL wind tunnel is a closed-circuit wind tunnel with a boundary-layer test section 20 m long, 2.4 m wide and 2.3 m high, optically transparent side walls, and with a capacity of generating a maximum wind speed of 40 m/s in the test section. Arrays of chains were laid-out on the wind tunnel’s floor on the upstream side of the wind turbine model in order to match the flow to that of offshore environment. The boundary layer growth of the simulated ABL wind under almost zero pressure gradient condition was achieved by adjusting the ceiling height of the test section of the wind tunnel. The oncoming boundary layer wind velocity profile was fitted by using Equation 1, where y_{ref} is a reference height (hub) and U_{ref} is the wind speed at the reference height. The power law exponent ’α’ is associated with the local terrain roughness. Figure 1, shows the measured stream-wise mean velocity (normalized with respect to the hub height velocity, U_{hub}) and the turbulence intensity profiles of the oncoming flow in the test section for the present study. The power law exponent in Equation 1 was found to be α = 0.10, corresponding to the open sea boundary layer profile according to the Japanese standard (AIJ or Architecture Institute of Japan). GL (Germanischer Lloyd) regulations define a turbulence intensity of 0.12 at the hub height of offshore wind turbines; however, this value was determined to be very conservative compared to field measurements. However, the values of α, and the turbulence intensity for offshore locations are site specific and they can vary greatly depending on whether we are talking about the near coast or open seas. For the current experimental study, a turbulence intensity of 10% at the hub height of the model turbine was chosen.

$$\frac{U}{U_{ref}} = \left(\frac{y}{y_{ref}}\right)^{\alpha} \tag{1}$$

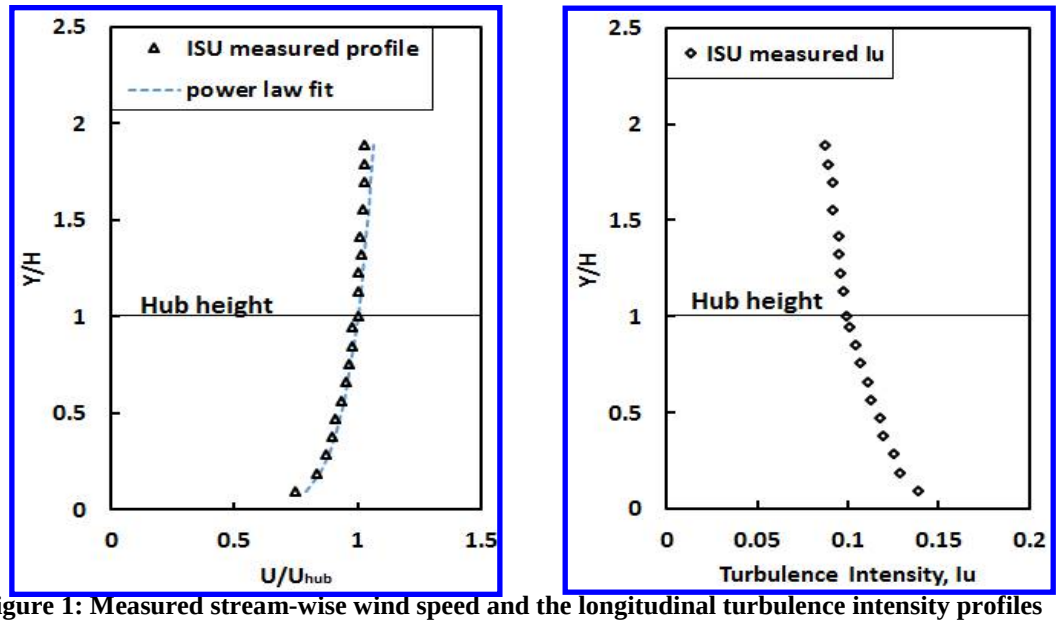

Figure 1: Measured stream-wise wind speed and the longitudinal turbulence intensity profiles

Figure 2 shows, a 1:300 geometrically scaled model horizontal axis wind turbine (HAWT) of height 270 mm (81m in full scale) measured from the wind tunnel's floor to the hub height of the turbine. However, the base of the turbine's tower was extended beyond the tunnel's floor to connect it to the motion simulator fixed underneath the tunnel (an additional height of 130mm). The rotor diameter for this scaled model was chosen as 300 mm (90m in full scale), and the turbine was developed using rapid prototyping method. The rotor blades were designed based on the ERS-100 prototype turbine blades developed by TPI Composites, Inc. The rotor blade has a constant circular cross section from the blade root to 5% blade radius (R), and three NREL airfoil profiles (S819, S820, S821) were used at different span-wise locations along the rotor blade. The S821 airfoil profile spans between 0.208R and 0.40R, the S819 primary airfoil is positioned at 0.70R, and the S820 airfoil profile is specified at 0.95R. For optimal performance of the rotor, the blades were pitched by 3 degrees.

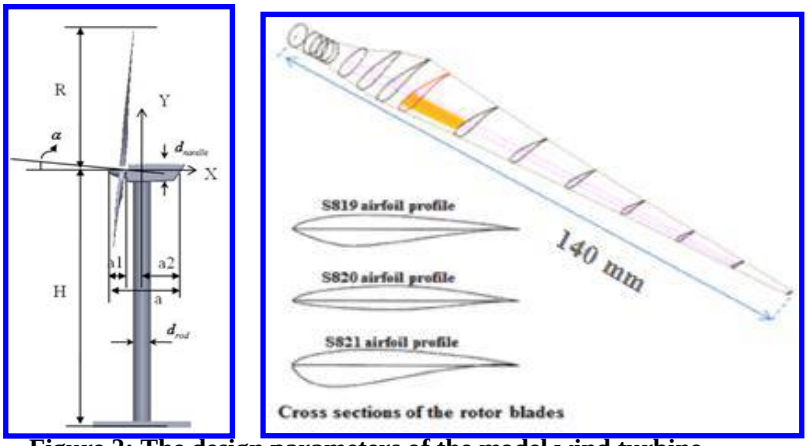

Figure 2: The design parameters of the model wind turbine

The blockage ratio was calculated to be around 1.3%, which is well within the acceptable limit of 5%. The incoming velocity, U_∞,was set to 3.5m/s at the hub height of the turbine that provided a rotational speed of 17 Hz for the model turbine. The Reynolds number corresponding to the prototype wind turbines range between 500,000 to 6,000,000. However, the corresponding diameter based Reynolds number (Re_D) for this experiment was 71000 which was much lower than that of the large-scale wind turbines operating in the fields.

A tip-speed-ratio (TSR) of 4.5 was maintained throughout the test. The tip-speed-ratio, is the ratio between the rotational velocity of the turbine to the free-stream velocity.

$$\mathrm{TSR} = \frac{\Omega R}{U_\infty} \tag{2}$$

where Ω is the angular velocity of the model turbine in rad/s.

Besides matching the TSR between the model and the prototype wind turbines, other scale relationships must also be maintained when dealing with floating wind turbines (Martin et al, 2012). Froude number is the ratio between the inertial to gravitational forces. Matching Froude scale ($\lambda_{Fr} = 1$), is the method of choice when dealing with hydrodynamic testing of scaled model floating wind turbines.

By using Froude scaling, the wave forces and response of the floater will be correct (ignoring the scale effect in viscous forces). The wind loads on the turbine should also be scaled using Froude scaling, otherwise the floater motions will not be correct. In hydrodynamic testing, this is achieved by calibrating the correct wind forces, rather than the correct wind velocity. Therefore, once the Froude scaling is applied to the wind velocity, further adaptation of wind velocity will be required in order to achieve an acceptable thrust load on the turbine.

However, in wind tunnel model study of offshore wind turbine, the Froude scaling may not be an appropriate similitude method. This is mainly because the wind speed need to be adjusted to obtain the correct wind loads on the turbine, if the range of motions on the scaled model turbine as determined using Froude scaling is to be maintained. Therefore, matching Froude number would not be able to accurately capture the characteristics of a floating turbine that is subjected to base motions.

A scaling method termed here as velocity ratio method was therefore chosen for the current study in order to capture the important characteristics of the wake of the turbine subjected to pitch motions. The velocity ratio method was achieved by maintaining the ratio between the maximum velocity of the pitch motion to the freestream velocity for both the model and the prototype.

$$\left(\frac{U_{\mathrm{pitch}}}{U_\infty}\right)_{\mathrm{prototype}} \sim \left(\frac{2Af}{U_\infty}\right)_{\mathrm{model}} \tag{3}$$

Where A is the amplitude of displacement and f is the frequency of oscillation in Hz for the pitch motion. The motion simulator devices that were used for the current experimental study includes a URS50BCC (for pitch) high precision rotation stages motion simulator manufactured by Newport Corporations and was used to replicate the pitch motions of a floating wind turbine. As can be seen in Figure 3, the motion simulator device was carefully installed under the test section floor of the wind tunnel to avoid any flow disturbances due to the presence of such device. The turbine was then placed on top of the motion simulator through a special cut in the tunnel's floor, to prevent the air from leaking out of the tunnel.

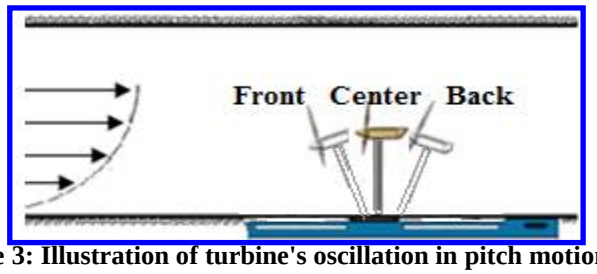

Figure 3: Illustration of turbine's oscillation in pitch motion.

A 2-D Particle Image Velocimetry (PIV) technique was used (as shown in Figure 4) to capture whole-field information of the wake of both the bottom fixed turbine and the turbine with the pitch motion. The coordinate system indicating three velocity components is also shown in Figure 10. The flow was seeded with 1-5 μm oil droplets and the laser system used for illumination of the seeding particles was a double-pulsed Nd:YAG laser (Ever Green big sky laser series) emitting two 200 mJ laser pulses at a wavelength of 532 nm and with a repetition rate of 1 Hz. For a better accuracy in results, the laser sheet thickness was adjusted to be around 1 mm. Two high-resolution

(2048×2048 pixels) charge-coupled device (CCD) cameras with axis perpendicular to the laser sheet was used for PIV image acquisition. The CCD camera and the double-pulsed Nd:YAG lasers were connected to a workstation via a digital delay generator that controlled the timing of both the laser illumination and the image acquisition.

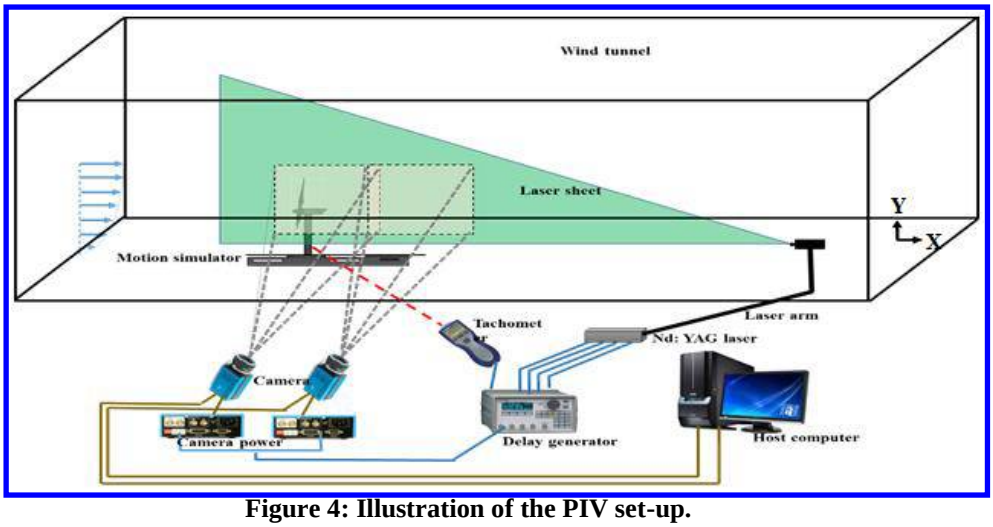

Figure 4: Illustration of the PIV set-up.

Instantaneous PIV velocity vectors were obtained using a frame-to-frame cross correlation technique involving successive frames of patterns of particle images in an interrogation window with 32×32 pixels and an effective overlap of 50% to satisfy the Nyquist criterion. The ensemble averaged flow quantities such as mean velocity, turbulent-velocity fluctuations, normalized turbulent kinetic energy, and Reynolds shear stress distributions were obtained from approximately 1000 frames of instantaneous PIV measurements. The measurement uncertainty level for the velocity vectors was estimated to be within 2.0%, and that of the turbulent velocity fluctuations and turbulent kinetics energy was about 5.0%.

As shown in Figure 3, the x-coordinate corresponds to the stream-wise direction with the origin located at the center of the tower of the turbine. The y-coordinate which is in lateral direction (pointing towards the ceiling), with its origin at the center of the nacelle. Using the right hand rule, the z-coordinate would then be perpendicular to the x-y plane and will be pointing to the right side of the wind tunnel's wall.

III. Results and Discussions

Out of the six degrees of freedom associated with any floating offshore wind turbines, the pitch motion is believed to be the most dominant motion. As can be seen in Figure 3, the pitching motion is defined as the angular motion of the turbine along the wind direction (the stream-wise). The exact motions for the prototype turbine in pitch motion for the current study were determined using the previous numerical simulations results done on floating wind turbines. For the current study, the freestream velocity at the hub height of the scaled model turbine was set to 3.5 m/s. The turbine was pitched from -5 degrees to +5 degrees. The pitching speed at the base of the tower was set to the maximum amount that the motion simulator could perform to 20 $\frac{\text{deg}}{\text{s}}$ which resulted in a frequency of 0.3 Hz.

As previously described, a JR3 force-moment transducer was used in the present study that can provide the time-resolved measurements of all three component of the aerodynamic forces and moments about each axis. However, for the current study of the wind loads acting on turbine unit, static or dynamic, only the axial wind loads were considered, while other components of the loads can also be important factor in designing wind turbines and the floating platforms. Figure 5, gives the wind load measurement results in term of the instantaneous thrust coefficients for both the bottom fixed turbine and the moving turbine in pitch motion. As can be clearly seen from the time histories of the measured instantaneous thrust forces given in Figure 5, these loads are highly unsteady with their magnitudes fluctuating significantly as a function of time. The wind loads acting on the bottom fixed turbine in Figure 5(a), were found to be significantly different to the loads seen by the turbine in pitch motion 5(b). While the

mean value of the wind loads acting on the turbine in pitch motion (i.e., C_T =0.3701) is slightly higher than that of the bottom fixed turbine (i.e., C_T =0.3647), the fluctuation amplitudes of the pitching motion were found to be significantly higher, which consequently increases the fatigue loads and ultimately reduces the life time of the moving turbine and the corresponding mooring lines of the floating platform which holds the turbine.

Figure 6 corresponds to the power spectral density of the measured instantaneous thrust forces acting on both model wind turbines (i.e. bottom fixed turbine and the oscillating turbine in pitching motion) through a Fast Fourier Transform (FFT) analysis procedure. In the case of the bottom fixed turbine (i.e. red color), a dominant peak at f_0 = 17 Hz can be identified which corresponds to the rotational speed of the turbines rotor blades at the optimum tip-speed-ratio of 4.5. The rotational frequency of f_0 = 17 Hz based on FFT analysis of the dynamic wind load measurements was found to agree very well with the independently measured rotational speed of the turbine blades by using a tachometer. However, in the case of the oscillating turbine in pitch motion, multiple dominant frequencies are observed. As the turbine was oscillating with a very low frequency, the power spectra plot clearly shows a dominant frequency of 0.3 Hz. As the turbine was oscillating in pitch motion, the relative velocity seen by the rotor and the effective angle of attack of the blades significantly change, contributing to significant fluctuations in the rotational frequency of the rotor are apparent in the power spectra plot.

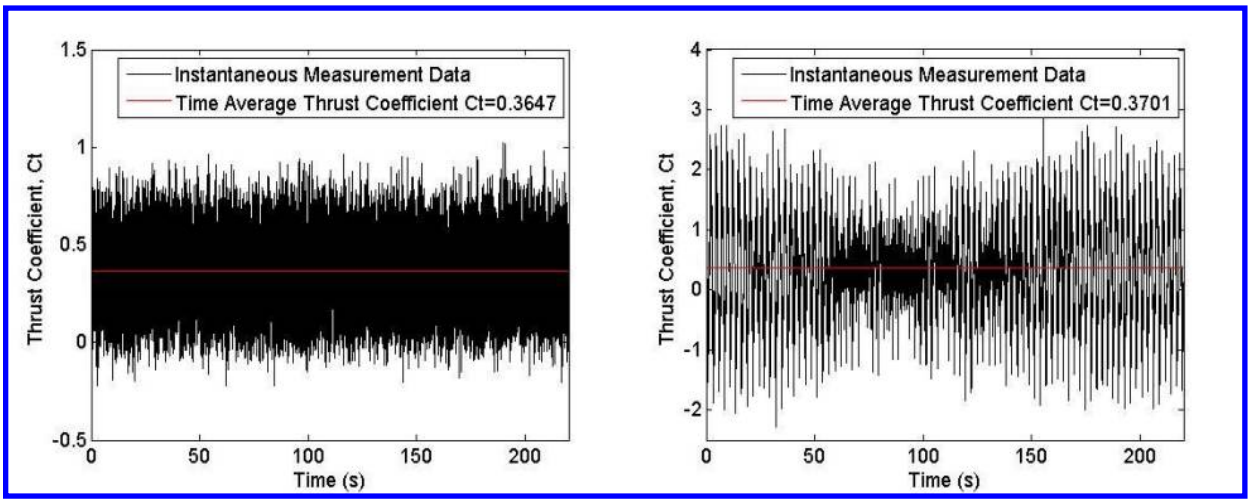

Figure 5: Measurement results of dynamic thrust force acting on the model wind turbine. Left (5a): bottom fixed turbine. Right (5b): turbine in pitch motion.

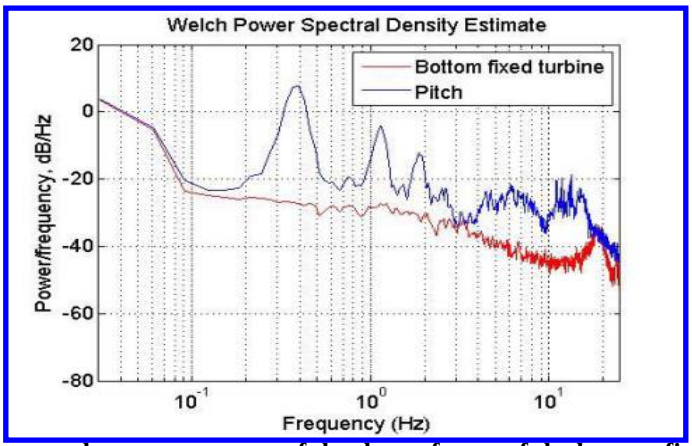

Figure 6: Comparison between the power spectra of the thrust forces of the bottom fixed turbine and the oscillating turbine in pitch motion.

The turbine's power efficiency was determined using the voltage output of a small DC generator installed in the nacelle of the wind turbine. Many studies have been done to understand the effects of the ambient turbulence intensity on the loading, performance, and wake patterns of horizontal axis wind turbines. Power losses due to the wake effects can reach up to 23% depending on the spacing and alignment of wind turbines [17]. Field measurements at Horns-Rev offshore wind farm revealed nearly 20% recovery on the maximum power deficit of the downstream turbines at higher ambient turbulence levels [20]. Barthelmie et al [16], also estimated that wind farm efficiency at Nysted wind farm will improve up to 9% in unstable conditions with higher ambient turbulence levels.

In a wind tunnel study performed by Ozbay et al [14], an increase of 6% was reported in the power output of an onshore wind farm over a similar layout corresponding to offshore scenario and concluded that the higher ambient turbulence intensity is solely responsible for such phenomena. The analysis done by Chamorro and Porte-Agel [5], shows strong dependence between the velocity deficit and the atmospheric turbulence.

Figure 7, shows the normalized power output of the bottom fixed turbine and the pitching turbine. As can be seen in Figure 7, there is little difference between the mean power extractions by the two turbines. However, as can clearly be seen in Figure 8, the fluctuations in the power extraction of the pitching turbine is substantially higher than those of the bottom fixed turbine. It is important to note that these fluctuations will significantly impact the quality of power generated by such oscillating turbines.

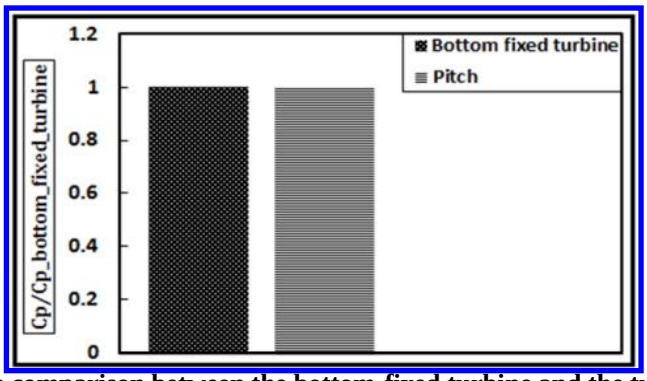

Figure 7: Performance comparison between the bottom-fixed turbine and the turbine in pitch motion.

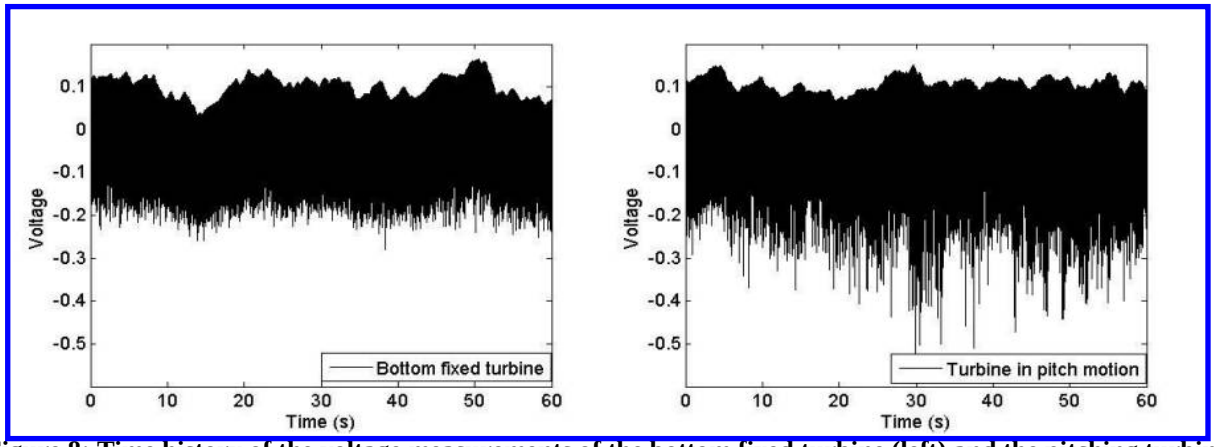

Figure 8: Time history of the voltage measurements of the bottom fixed turbine (left) and the pitching turbine (right).

The flow field (x/D < 1.8) measurement in the wake of the pitching turbine was also carried out by using a high-resolution PIV system, and the wake results obtained at the center location were then compared to those of a classical bottom-fixed turbine.

The flow measurements were used to quantify the differences in the wake of the pitching turbine when the aerodynamic hysteresis occurs. In the hysteresis loop, the differences in the wake flow at the same pitching

condition were examined along the increasing pitch angle (i.e., the turbine is pitching *with the flow*) and the decreasing pitch angle (i.e., the turbine is pitching *into the flow*) branches.

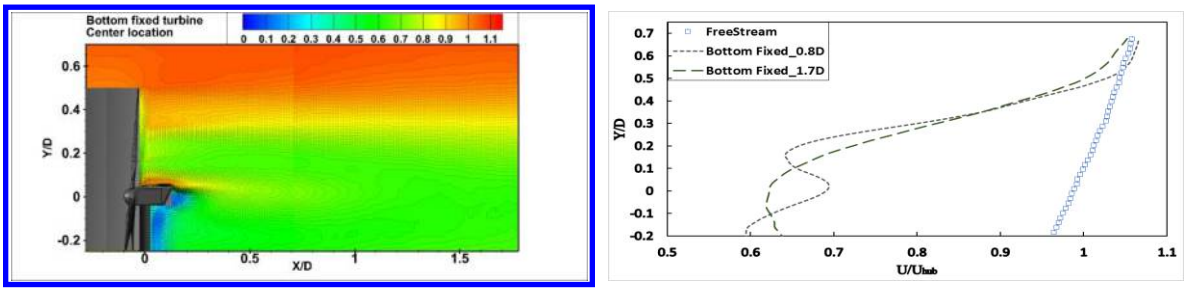

(a) Bottom Fixed Turbine – U/Uhub – Center location

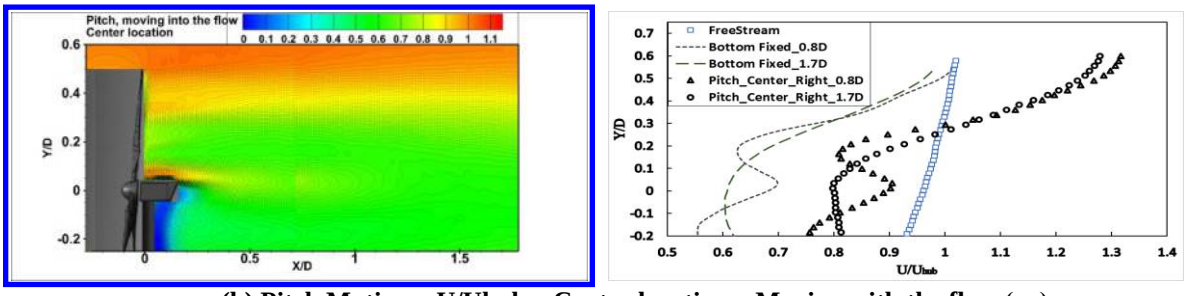

(b) Pitch Motion – U/Uhub – Center location – Moving with the flow (→)

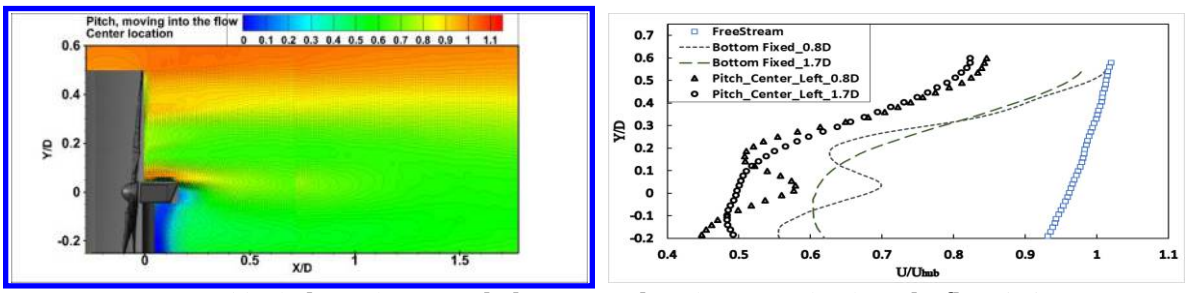

(c) Pitch Motion – U/Uhub – Center location – Moving into the flow (←)

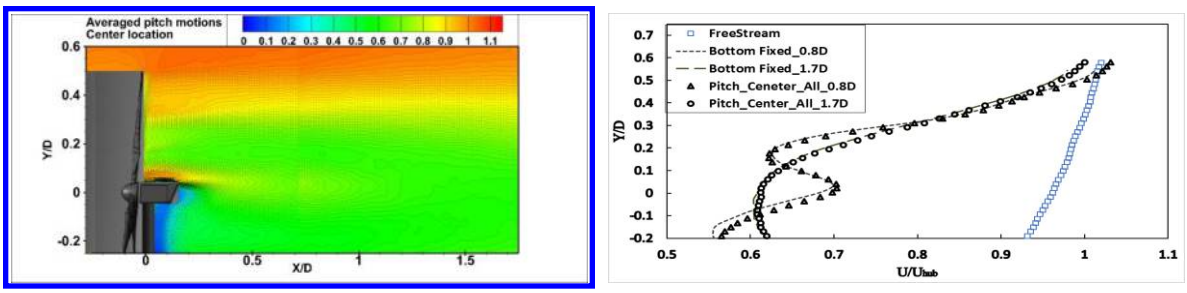

(d) Pitch Motion – U/Uhub – Center location – Averaged motion

Figure 9: Normalized stream-wise velocity (U/Uhub) profiles in the wake of a bottom fixed turbine (a), the center location for a pitching turbine as it is moving with the flow (b), as it is moving into the flow (c), and the averaged of forward and backward motion (d).

The measurement plane was composed of two fields with an overlap of 15mm length, and two CCD cameras were used to acquire images from these fields. Two fields were then merged in Tecplot to acquire the image in the measurement plane. Finally, ensemble averaged flow quantities, such as mean flow velocity, Reynolds stresses and Turbulence Kinetic energy, were analyzed.

Figure 9, shows the four pairs of contour plots accompanied by their extracted data (at x/D = 0.8 and x/D=1.7) of the PIV measurements of the averaged stream-wise velocity component U, normalized by the relative velocity experienced by the rotor at the hub height, for a classical bottom fixed turbine (a), the pitching turbine at the center location (0°) when moving with the flow (b), moving into the flow (c), and the ensemble averages of the forward and backward motions at the center location (d).

As can be seen in Figure 9, there is clear evidence of the deficit in the velocity in the wake of both; the bottom fixed turbine and the pitching turbine. This deficit is the result of energy extraction by the turbine itself. Double peaks are observed and understood as characteristic of the near wake profiles (X/D <1). But as we go farther down in the wake (X/D >1), the double peaks die out and become just a single peak. This single peak eventually dies out in approximately 15~20 diameter downstream of the turbine, where the flow gains its fullest momentum and becomes the undisturbed flow again. There is some overshoot at the top region of the profiles in the near wake regions which suggests that the flow is accelerating at near top-tip of the blade, and also could be an evidence of the blockage effect caused by the existence of the turbine itself.

From the extracted data of Figure 9b and 9c, during the pitching motion, as the turbine is at the center location and is moving with the flow (to the right), it's wake tends to accelerate when compared to the wake of the bottom fixed turbine, suggesting a reduced energy extraction by the rotor. This trend is anticipated to become more pronounced as we go down farther in the wake. However, as the turbine is moving into the flow (to the left), the wake of the pitching turbine slows down in comparison to the bottom fixed turbine, suggesting an increase energy extraction by the rotor from the flow. When averaging both motions, there would be no difference between the wakes of the bottom fixed turbine and the pitching turbine (9d), suggesting an equal amount of power extraction by both turbines.

Sebastian et al. (2013), performed series of numerical simulations on floating wind turbines, and determined that the blade element momentum theory (BEM) does not capture the unsteadiness generated in the flow due to significant changes in the angle of attack. Large angle of attack changes were due to the additional motion of the floating platforms. Motion induced unsteadiness violates assumptions of standard blade element momentum theory and leads to inaccurate predictions of unsteady aerodynamic loads. He showed that pitching motion of the wind turbine causes the turbine to change from the windmill state to the propeller state.

Figure 10, shows the Reynolds shear stress ($\tau = \frac{-u'v'}{U_{hub}^2}$) and the turbulent kinetic energy ($T.K.E. = \frac{1}{2}\frac{[u'^2+v'^2]}{U_{hub}^2}$). The Reynolds shear stress deals with the transport of momentum from high energy flow above the rotor to the lower energy area of the wake region. T.K.E. is the kinetic energy per unit mass associated with the eddies in the turbulent flows. T.K.E. deals with the diffusivity effect which is responsible for enhanced mixing. By studying both the Reynolds shear stress and the T.K.E., one can determine on how fast the wake is recovering. The fluctuating components of the oncoming boundary layer flow influences the turbulent wake flow structure significantly. For a uniform flow, mean shear distribution in the turbine wake could be axisymmetric with strong shear layer (associated with TKE production) at the levels of bottom-tip and top-tip. However, for an oncoming boundary layer flow with non-uniform mean flow velocity distribution, previous experimental and numerical studies showed that maximum TKE production would occur at the top-tip level as a result of strong shear-produced turbulence and turbulent fluxes (Hu et al., 2012; Zhang et al., 2012; Porte-Agel et al., 2011; Wu et al., 2012). Turbulent fluxes produced due to wake induced turbulence were found to play an important role on the entrainment of energy from the flow above the wind farm (Meyers and Meneveau, 2013).

As can be seen in Figure 10, there are relatively higher amount of Reynolds shear stress, and T.K.E. associated with the pitching turbine, as it is moving into the flow when compared to the bottom fixed turbine, and lower amount associated with the pitching turbine moving with the flow. This is an indication of faster wake recovery as the turbine is oscillating into the flow and slower wake recovery when the turbine in pitching with the flow. However, when averaging both motions (10d), there would be little difference between the wake recovery of a bottom fixed turbine and a pitching turbine.

Rockel et al. (2014) also found that the classical bottom fixed turbine with its rigid structure would enhance mixing thereby providing a faster recovery in the shear layer of the wake when compared to the pitching turbine. Therefore, the far wake region behind the fixed turbine and the pitching turbine would significantly differ, affecting

the performance of the downwind turbines operating in the wake of the front row turbines. The power extracted by the downwind pitching turbines would be 14% - 16% lower (with front row turbines pitching to approximately 18°) than the turbines behind the bottom-fixed turbine.

However, recent study showed that the reduced range of the pitching angle for the floating turbine would provide almost the same far wake velocity pattern as for the bottom-fixed turbine. Therefore, downwind turbines behind the fixed and pitching turbine would perform almost the same.

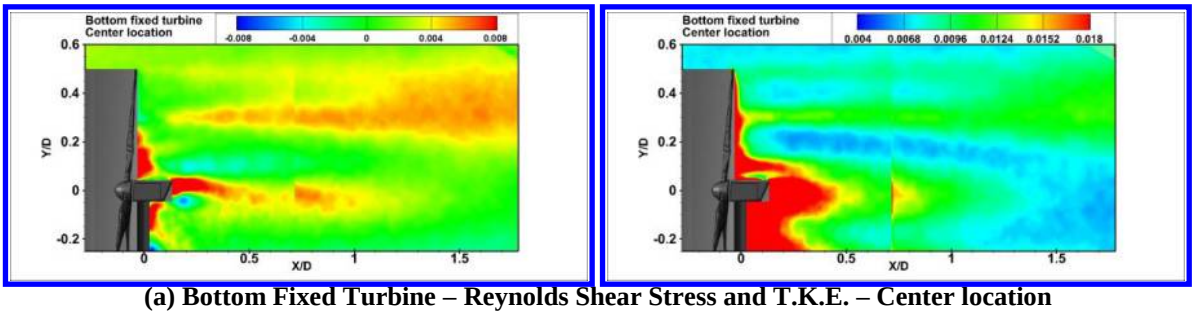

(a) Bottom Fixed Turbine – Reynolds Shear Stress and T.K.E. – Center location

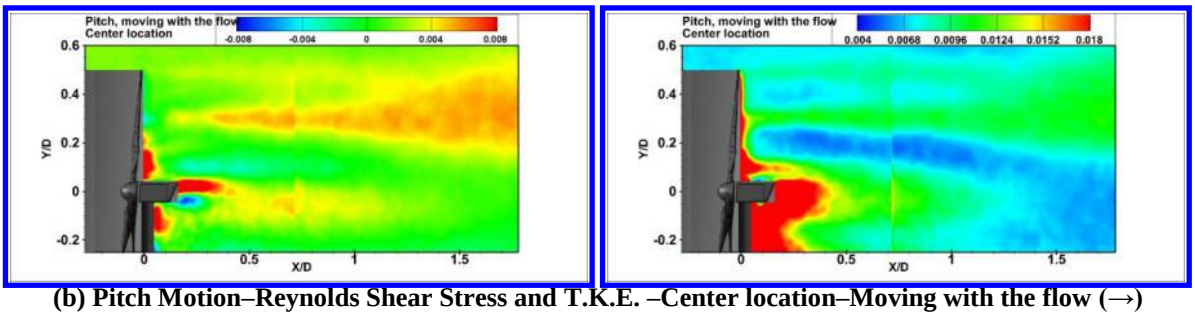

(b) Pitch Motion–Reynolds Shear Stress and T.K.E. –Center location–Moving with the flow (→)

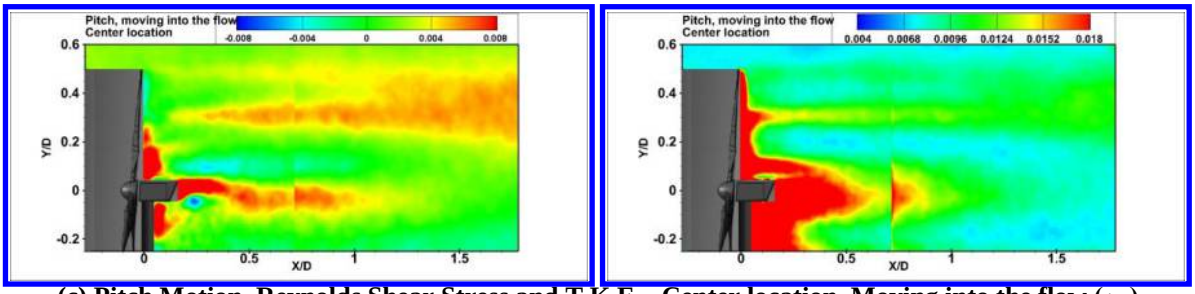

(c) Pitch Motion–Reynolds Shear Stress and T.K.E. –Center location–Moving into the flow (←)

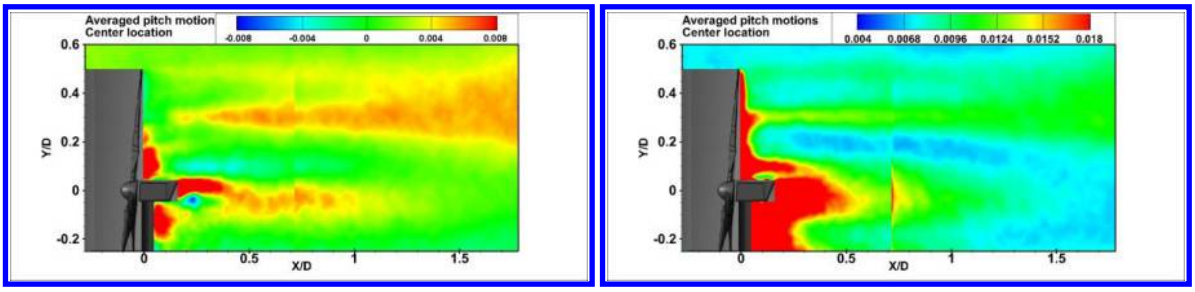

(d) Pitch Motion–Reynolds Shear Stress and T.K.E. –Center location–Averaged Both Motion (◄►)

Figure 10: Normalized Reynolds Shear Stress ($\frac{Ruv}{U_{hub}^2}$) and the Turbulent Kinetic Energy ($\frac{T.K.E.}{U_{hub}^2}$) plots in the wake of a bottom fixed turbine (a), and the center location of a pitching turbine as it is moving with the flow (b), as it is moving into the flow (c), and the averaged of forward and backward motion (d).

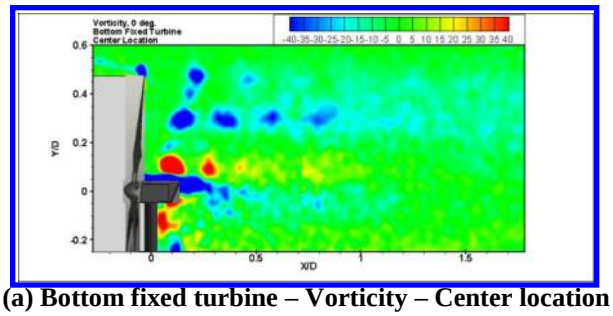

(a) Bottom fixed turbine – Vorticity – Center location

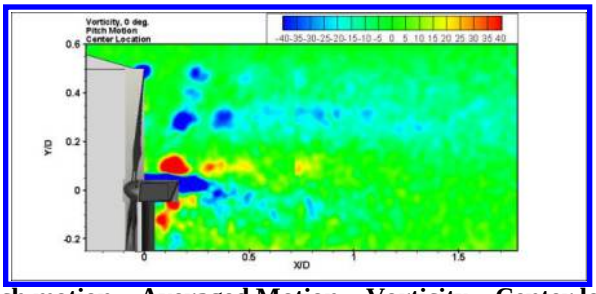

(b) Pitch motion – Averaged Motion – Vorticity – Center location

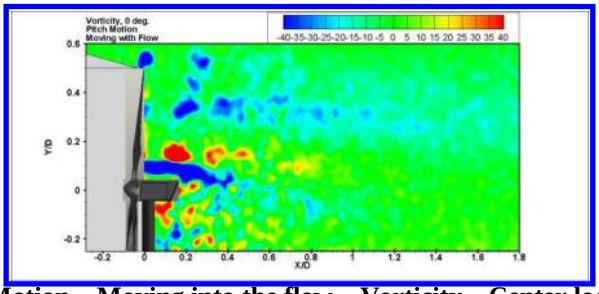

(c) Pitch Motion – Moving into the flow – Vorticity – Center location (→)

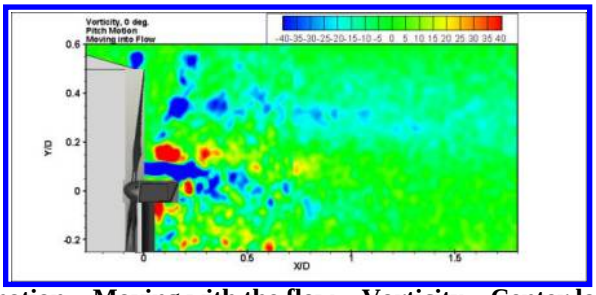

(d) Pitch motion – Moving with the flow – Vorticity – Center location (←)

Figure 11: Normalized vorticity distribution $(\frac{w_z D}{U_{hub}})$ plots in the wake of a bottom fixed turbine (a), and the center location for the pitching turbine: the averaged vorticity of forward and backward motions (b), as it is moving with the flow (c), and as it is moving into the flow (d).

Figure 11, shows the normalized phase-locked $(\frac{w_z D}{U_{hub}})$ vorticity distributions in the wake of the bottom fixed turbine and the turbine oscillating in pitch motion at a phase angle of $\theta = 0°$. The vorticity (w_z) values were derived from the phase locked velocity distributions in the streamwise and vertical directions by using the expression

$w_z = \frac{dv}{dx} - \frac{dU}{dy}$. The phase-locked PIV measurements could be used to identify the unsteady vortex structures (i.e., tip and root vortices, and vortices formed within the nacelle boundary layer) generated in the wake.

As shown in Figure 11, the tip vortices were formed in the strong shear layer located at the uppermost level of the wake. Interestingly, an additional array of concentrated vortices were found to shed from the inboard section located at approximately 50% - 60% of the blade span. Furthermore, these vortex structures were found to expand outwards as they convect downstream and finally merge with those shedding from the blade tips. Moreover, these additional array of concentrated vortices were found to be larger and stronger than those generated by the blade tips. The vortices formed within the nacelle boundary layer with those shedding from the blade root section were found to dissipate much faster than those generated at the tip and inboard section of the blade.

There is a strong connection between the tip vortex breakdown and the shear layer expansion. Lignarolo et al. (2013) showed that tip-vortices could act against the turbulent mixing; however, the break-down of these vortices could enhance turbulent mixing.

The effect of the hysteresis loop on the evolution (i.e., formation, shedding and dissipation) of the unsteady vortex structures for the bottom fixed turbine and the oscillating turbine are shown in Figure 28. The hysteresis loop was found to make no significant changes on the evolution of the unsteady vortex structures. However, slight changes in the shape and magnitude of the vortex structures can be seen. Furthermore, contrary to the bottom fixed turbine, the vortices shedding from the inboard and tip sections of the turbine blade were found to break-down/dissipate faster for the oscillating turbine. However, the behavior of the vortices shedding from the nacelle boundary layer and blade root section was pretty similar for the fixed and the turbine in pitching motion.

IV. CONCLUSION

A comprehensive experimental study was conducted to investigate the performance, loading and the near wake characteristics of a horizontal axis wind turbine subjected to pitch motions. The results were then compared to those of a classical bottom fixed turbine. The current study was performed in a large-scale atmospheric boundary layer wind tunnel. The base of a 1:300 scaled model wind turbine was mounted on a translation stage. The rotation stage was controlled to generate surge motions to simulate the dynamic pitch motions experienced by floating offshore wind turbines. During the experiments, the velocity scaling method was chosen to maintain the similar velocity ratios (i.e., the ratios of the incoming airflow flow to that of turbine base motion) between the model and the prototype.

During the experiments, a high resolution digital particle image velocimetry (PIV) system was used to achieve flow field measurements to quantify the characteristics of the turbulent vortex flow in the near wake of the wind turbine model. Besides conducting ‘‘free run’’ PIV measurements to determine the ensemble-averaged statistics of the flow quantities such as mean velocity, Reynolds stress, and turbulence kinetic energy (TKE) distributions in the wake flow, ‘‘phase-locked’’ PIV measurements were also performed to elucidate further details about evolution of the unsteady vortex structures in the wake flow in relation to the position of the rotating turbine blades.

The results of the wake study reveals that the wake of a wind turbine subjected to pitch motions, is highly dependent on which direction the turbine is oscillating. Furthermore, the velocity, frequency, and the range of oscillation also play an important role on the behavior and the wake pattern of the moving turbine. The wake of the oscillating turbine in pitch motion, tends to accelerate as the turbine is moving with the flow, hence, reducing the power extraction by the turbine. A decrease in Reynolds shear stress and the turbulent kinetic energy production was noted as the turbine was oscillating with the flow. However, as the turbine was moving into the flow, these effects reverse, and causes a deceleration in the wake of the moving turbine, hence increases the power production by the turbine, and increases the Reynolds shear stress and the turbulent kinetic energy. Averaging the wake results of both forward and backward motions of the turbine in pitch motion produces results which are essentially the same as the wake pattern of the bottom fixed turbine.

Although, the mean power measured by a small DC motor installed in the nacelle shows little difference between the oscillating turbine and the bottom fixed turbine, but the excessive fluctuations in the power output of the oscillating turbine is anticipated to greatly reduce the power quality of such oscillating turbines. The load measurements also show substantial amount of increase in terms of the fluctuating components for the oscillating turbine, which consequently results in increased fatigue loads and decreased lifetime of the turbine and the associated floating components.

ACKNOWLEDGMENT

This research work is funded by National Science Foundation under the Grant No. 1438099 and 1069283 which supports the activities of the Integrative Graduate Education and Research Traineeship (IGERT) in Wind Energy Science, Engineering and Policy (WESEP) at Iowa State University.

References

Sebastian, T.; Lackner, M. Characterization of the unsteady aerodynamics of offshore floating wind turbines. Wind Energy 2013, 16, 339–352.

Rockel, S.; Camp, E.; Schmidt, J.; Peinke, J.; Cal, R.B.; Hölling, M. Experimental Study on Influence of Pitch Motion on the Wake of a Floating Wind Turbine Model. Energies 2014, 7, 1954-1985.

Vermeer LJ, Sorensen JN, Crespo A (2003) Wind turbine wake aerodynamics. Prog Aerosp Sci 39:467–510

Massouh H, Dobrev I (2007) Exploration of the vortex behind of wind turbine rotor. J Phys Conf Ser 75:012036

Chamorro, L. P., Porte-Agel, F. (2009). A wind-tunnel investigation of wind-turbine wakes: boundary layer turbulence effects. Boundary Layer Meteorol 132:129–149

Porte-Agel, F., Wu, Y. T., Lu, H., Conzemius, R. J. (2011). Large-eddy simulation of atmospheric boundary layer flow through wind turbines and wind farms. Journal of Wind Engineering and Industrial Aerodynamics, 99, 154–168.

Zhang, W., Markfort, C. D., Porte-Agel, F. (2012). Near-wake flow structure downwind of a wind turbine in a turbulent boundary layer. Experiments in Fluids, *52*, 1219–1235.

Hu, H., Yang, Z., Sarkar, P., (2012). Dynamic Wind Loads and Wake Characteristics of a Wind Turbine Model in an Atmospheric Boundary Layer Wind. *Experiments in Fluids 52*(5):1277-1294.

Wu, Y. T. & Porte-Agel, F. (2012). Atmospheric turbulence effects on wind-turbine wakes: An LES study. Energies, *5*, (12), 5340–5362.

Musial W., Ram B., 2010, Large-Scale Offshore Wind Power in the United States, Technical Report NREL/TP-500-40745.

Martin H.R., 2011, Development of a Scale Model Wind Turbine for Testing of Offshore Floating Wind Turbine Systems, M.S. Thesis, University of Maine, Orono.

Wieringa, J (1992). Updating the Davenport roughness classification. Journal of Wind Engineering and Industrial Aerodynamics 41-44, 357-386.

Manwell, J. F., McGowan, J. G., & Rogers, A. L. (2010). Wind Energy Explained: Theory, Design and Application, 2nd edition. Wiley.

Hau, E. Wind Turbines Fundamentals, Technologies, Application, Economics, 2nd edition. Springer

A. Ozbay, W. Tian, Z. Yang, and H. Hu, "An experimental investigation on the wake interference of multiple wind turbines in atmospheric boundary layer winds," in AIAA-2012-2784, 30th AIAA Applied Aerodynamics Conference, New Orleans, Louisiana, 25-28 June 2012

Corbetta, G., Mbistrova, A. 2015, The European offshore wind industry key trends and statistics 2014, EWEA.

K. S. Hansen, R. J. Barthelmie, L. E. Jensen, and A. Sommer, "The impact of turbulence intensity and atmospheric stability on power deficits due to wind turbine wakes at Horns Rev wind farm," Wind Energy 15, 183–196 (2012).

Sanderse, B. (2009). Aerodynamics of wind turbine wakes: Literature review. Energy Research Center of the Netherlands (ECN).

Lignarolo, L.E.M., Ragni, D. Krishnaswami, C., Chen, Q., Simao Ferreira, C. J., & Van Bussel, G.J.W. (2013). Experimental analysis of the kinetic energy transport and turbulence production in the wake of a model wind turbine. ICOWES Conference, Lyngby, 16-19 June.

Architecture Institute of Japan, AIJ Recommendations for Loads on Buildings (Architectural Institute of Japan, 1996).

Barthelmie, R. and Jensen, L. E. (2010). Evaluation of the wind farm efficiency and wind turbine wakes at the Nysted offshore wind farm. Wind Energy, 13:573-586. Doi:10.1002/we.408

Barthelmie, R. J., Hansen, K., Frandsen, S.T., Rathmann, O., Schepers, J.G., Schlez, W., et al. (2009). Modeling and measuring flow and wind turbine wakes in large wind farms offshore. Wind Energy 12(5), 431-444. Doi:10.1002/we.348.

Meyers, J., & Meneveau, C. (2013). Flow visualization using momentum and energy transport tubes and applications to turbulent flow in wind farms. Journal of Fluid Mechanics 715, 335-358.

J.M. Jonkman, (2007). Dynamics Modeling and Loads Analysis of an Offshore Floating Wind Turbine Technical Report NREL/TP-500-41958

Cal, R. B., Lebron, J., Castillo, L., Kang, H.S., Meneveau, C. (2010). Experimental study of the horizontally averaged flow structure in a model wind-turbine array boundary layer. J Renew sustain Energy 2:013-106.